Journal of Pharmaceutical Sciences 000 (2024) 1–10

Contents lists available at ScienceDirect

Journal of Pharmaceutical Sciences

journal homepage: www.jpharmsci.org

Pharmaceutics, Drug Delivery and Pharmaceutical Technology

Impact of surfactants on solution behavior and membrane transport of amorphous solid dispersions

Amjad Alhalaweh[a,c], Mira El Sayed[b,c], Lucia Kovac[c], Christel A.S. Bergström[b,*]

[a] College of Pharmacy, University of Sharjah, Sharjah, United Arab Emirates
[b] Department of Pharmacy, Uppsala University, Biomedical Centre, SE-751 23 Uppsala, Sweden
[c] Recipharm OT Chemistry AB, SE-754 50 Uppsala, Sweden

ARTICLE INFO

Article history:
Received 26 June 2024
Revised 11 October 2024
Accepted 11 October 2024
Available online xxx

Keywords:
Amorphous solid dispersion
Supersaturation
Solubility
Surfactant
Formulation

ABSTRACT

The purpose of the study was to develop an amorphous solid dispersion (ASD) of a poorly soluble compound (AK100) and investigate the impact of different surfactants on its dissolution, supersaturation and membrane transport. The solubility of the AK100 was determined in crystalline and amorphous form in the absence and presence of three surfactants at different concentrations: sodium dodecyl sulphate (SDS), polysorbate 80 (PS80) and D-α-tocopherol polyethylene glycol succinate (TPGS). The relation between solubility and surfactant solubilization was evaluated using a computational model. The ASD powder was prepared by solvent evaporation for non-sink dissolution experiments with and without the pre-dissolved surfactants. A transport study with Caco-2 cells was conducted to evaluate the impact of surfactants-based formulation on membrane transport. Both the corresponding crystalline and amorphous solubility of AK100 increased linearly as a function of the surfactant concentrations. The supersaturation was maintained for at least three hours in absence of surfactant and in presence of TPGS, whereas supersaturation declined with SDS and PS80. As expected, the membrane flux of the AK100 was higher for the ASD than for the crystalline powder, and further increased with increased concentration of TPGS. The supersaturation ratio based on the activity-based calculation from Caco-2 cells study was always higher than that of the concentration-based one for the amorphous and crystalline forms of AK100. This study shows how additional solubilizing excipients during formulation development can improve the resulting dissolution and phase behavior of supersaturated drug solution.

Introduction

Formulation of poorly soluble compounds remains a critical challenge for developing active pharmaceutical ingredients into medicinal products.[1,2] This process is even more difficult during the formulation development in early toxicology studies because they require a high dose of the compound to determine the toxicology profile.[3] Formulation scientists use various solubilization strategies to overcome poor solubility in drug formulation. These include solubilizing agents such as co-solvents, surfactants and complexing agents, pH adjustments, and lipid-based formulations.[4–6]

Oral delivery of solid dosage forms is the most preferred method of drug administration for several reasons, including ease of manufacturing, simplicity of administration, and patient safety.[7] This requires selecting the optimum solid form of the drug from a range of possibilities, such as the crystalline free form of the drug, its formulation with a salt, co-crystallization, or its amorphous state.[8] Traditionally, salts are used—when it is possible to synthesize them—as they often improve solubility. The salt form relies on ionization of the drug molecule and for non-ionizable drugs it is therefore often the crystalline form that is formulated with excipients to increase solubility. However, pharmaceutical cocrystals may be used to change the crystalline lattice to a more rapidly dissolving structure of non-ionizable drugs.[9] Although several studies show high solubility of cocrystals, the quick conversion of the cocrystal to the base form of the drug limits its further development.[10] The amorphous form has therefore gained in interest. It holds great potential if correctly stabilized and as reflected by the increased number of marketed products based on amorphous material.[11]

However, the amorphous material is thermodynamically unstable and therefore converts back to the stable crystalline form.[12] To respond to this challenge, there has been intensive research on amorphous materials to better understand their performance in the solid state and to find ways to stabilize them once formulated in a medicinal product. Polymers and other excipients can effectively stabilize

* Corresponding author.
E-mail address: christel.bergstrom@farmaci.uu.se (C.A.S. Bergström).

https://doi.org/10.1016/j.xphs.2024.10.023

drugs in their amorphous powder forms,[13] and are therefore often used in amorphous formulations of water-soluble compounds, mainly protein pharmaceuticals. However, the solution behavior of the amorphous material is an important feature in swift translation to oral medicinal products, and recent research has led to better understanding of the solution chemistry of amorphous material.[14,15] More importantly, the possibility to determine the maximum achievable concentration of the amorphous material gives formulation scientists the opportunity to engineer the amorphous formulation for maximum solubility.[16–18] The amorphous material increases the solubility of the drug by reducing the crystal lattice barrier, and the resulting increased thermodynamic activity improves membrane transport and thereby increases absorption and bioavailability.[15,19] The term amorphous "solubility" as used in this manuscript refers to the "apparent solubility" of the intrinsically unstable amorphous form of the drug.

The solution evolving from amorphous material is complex and affected by several factors. Among these are the temperature and the pH of the solution, and the presence of other excipients or components.[20]

Recent studies on the impact of polymer properties on the amorphous solid dispersion (ASD) behavior in solution have found that some polymers mix with the drug-rich phase that evolves in the liquid-liquid phase separation (LLPS).[21,22] This reduces the solubility of the drug as a result of the reduced chemical potential of the drug in solution. Crystallization behavior in the presence of different surfactants also differs, depending on the structure of the surfactant. Surfactants with unbranched hydrophobic tails enhance crystal nucleation more than those with bulky substituents.[21] Supersaturating formulations have also been studied for flux over an artificial membrane transport. Transport is reduced in the presence of surfactants or physiological fluids, being lower than expected from the dissolved amount of drug.[22,23] These studies also report that activity-based determination of supersaturation would better correlate with the performance of formulation, in particular with regards to the amount absorbed. Some studies have shown that the particle size of the nanoparticles evolving from amorphous formulation impact membrane transport of the drug and thus bioavailability.[24] Thus, formulation components such as surfactants and polymers may affect drug transport through the cell membrane. The effect of surfactants partitioning into the drug-rich phase and the enhanced crystallization can lead to negative impacts on drug transport across physiological membranes. However, surfactants might also act as absorption enhancers, counteracting the reduced transport caused by decreased thermodynamic activity.[25,26]

Membrane transport studies can be performed using artificial membranes, but absorption studies making use of Caco-2 monolayers are more physiologically relevant and can better predict *in vivo* formulation performance. This *in vitro* system makes it possible to evaluate the membrane transport of drugs before proceeding to *in vivo* animal studies, and can be used to further guide the solid form selection and potential formulation design.[27–29] In this study, we therefore set out to develop an amorphous solid dispersion of a poorly soluble model compound (AK100) with the purpose of investigating the impact of different surfactants on the resulting solution chemistry and dissolution of this formulation. These studies were concluded with absorption studies in Caco-2 cell monolayers to explore surfactant impact on membrane flux of the ASD.

Experimental section

Materials

The model compound (AK100) was supplied by Recipharm OT Chemistry (Uppsala, Sweden). Hydroxypropyl methylcellulose (HPMC): Shin-Etsu Hypromellose PHARMACOAT, Type AS-MF polymer was a gift from Shin-Etsu Chemical Co. (Tokyo, Japan). N, N-dimethyl acetamide (DMA), methanol, polysorbate 80 (PS80), and D-α-tocopherol polyethylene glycol 1000 succinate (TPGS) were purchased from Sigma-Aldrich (Stockholm, Sweden). Acetonitrile was purchased from Carlo Erba (Stockholm, Sweden). Dimethylsulfoxide (DMSO) and sodium dodecyl sulphate (SDS) from Apollo Scientific Ltd. (Manchester, UK). Dichloromethane (DCM) was obtained from Fisher Chemicals (Stockholm, Sweden). Octanol was provided by Chemtronica (Stockholm, Sweden). Milli-Q water was used for all aqueous solutions.

Methods

High performance liquid chromatography

The concentrations of AK100 were determined using an Agilent 1100 High Performance Liquid Chromatography (HPLC) system (Agilent Technologies, Santa Clara, CA) equipped with a DAD spectrometer detector. AK100 was separated on an XBridge C18 column (2.1 mm × 50 mm) with 5 μm particle size at 40 °C. The mobile phase was 60 % (v/v) acetonitrile and 40 % water, with a flow rate of 0.6 mL/min using an isocratic elution. The volume of injection was set to 5 μL and detection recorded at 300 nm. Calibration curves were constructed by analysing serial dilutions of a stock solution of the model compound; all exhibited good linearity ($R^2 \geq 0.99$).

Liquid chromatography–mass spectrometry (LC-MS)

The LC–MS/MS analysis of AK100 was performed on a Waters Quattro LC Micromass mass spectrometer (San Francisco, USA). Electrospray ionization (ESI) coupled with multiple reaction monitoring (MRM) mode was used. AK100 was separated on an XBridge C18 column as described above. The mobile phase consisted of 0.1 % (v/v) formic acid in acetonitrile and 0.1 % formic acid in water at a ratio of 25:75 and the flow rate was 0.4 mL/min. Spectra of AK100 between 210 and 600 nm were recorded with a Waters 2996 PDA. The injection sample volume was 50 μL, and the autosampler temperature was set to sample 15 °C with sample limit temperature 3 °C.

Differential scanning calorimetry

Differential Scanning Calorimetry (DSC) measurements were carried out using a TA Instrument Q1000 equipped with a refrigerated cooling system. The chamber was purged with a nitrogen at a flow rate of 50 mL/min during testing. The system was calibrated for temperature and enthalpy using indium and for heat capacity using sapphire. The thermodynamic parameters were calculated using TA Universal Analysis 2000 software. Samples (1–5 mg) were crimped into hermetic aluminium pans and an empty pan was used for reference. The onset of melting (T_m) and heat of fusion (ΔH_f) were determined using a heating rate of 10 °C/min for the AK100 and for the solid collected from the equilibrium solubility determination.

The glass transition temperature (T_g) of AK100 was determined by performing a heat-cool-heat cycle. First, the samples were heated to around 2 °C above the T_m using an equilibrate function. Then, the system was kept isothermal at this temperature for 2 min to ensure complete melting. Finally, it cooled to −20 °C at a ramp rate of 20 °C/min. The formation of a glassy state was then confirmed by the detection of a T_g on the thermograms upon heating the system again, at a heating rate of 20 °C/min, instantly after cooling. The ASD was studied by DSC using a heating rate of 20 °C/min.

Powder X-Ray diffraction

The Powder X-Ray Diffraction (PXRD) diffractograms were recorded using a Twin-Twin diffractometer (Bruker, Coventry, UK) measuring in Bragg–Brentano geometry and equipped with a sample rotator. The solid samples were placed on silicon sample holders during the measurement. The tube voltage and amperage were set to

40 kV and 40 mA, respectively. Cu Kα radiation (λ = 1.54 Å) was used in the measurements. A diffraction pattern in the 2θ range between 5° and 40° was collected at a scanning step of 0.02° and 0.3 s exposures. Primary and secondary divergence slits of 0.40 and 2.48 mm, respectively, were used.

Log P determination

To evaluate the lipophilicity of the AK100 model compound, the shake-flask method was used to determine the logarithm of the partition coefficient (log P) between octanol and water. The water phase was saturated with octanol and the octanol phase was saturated with water after which both phases were left to equilibrate and separate for at least 24 h. To 1.6 mL of the octanol-saturated water solution, 350 μl of water-saturated octanol and 50 μl of AK100 (0.25 mg/mL) in octanol were added. The mixture was shaken continuously for 3–4 h and then left to equilibrate for 72 h at room temperature. The octanol and water layers were separated, collected in vials and the AK100 concentration determined for each phase. HPLC was used for quantifying AK100 in the octanol phase. The concentration of dissolved drug in the water phase was too low to be detected by HPLC-UV, so LC-MS/MS was used instead. The equation for calculating log P was the following[30]:

$$\log P = \log\left(\frac{[AK100]_{octanol}}{[AK100]_{water}}\right) \quad (1)$$

where $[AK100]_{octanol}$ is the concentration of AK100 in the octanol phase and $[AK100_{water}]$ is the concentration of AK100 in the water phase.

Crystalline solubility determination

The equilibrium solubility of crystalline AK100 was determined by adding an excess amount ($\sim$ 5–7 mg) of the compound to 2 mL of water or water spiked with surfactant (SDS, PS80 or TPGS) at different concentrations Samples were placed in a room temperature under continuous shaking using a VWR Signature Multi-Tube shaker for 72 h. At least three independent experiments were performed. The supernatant was separated from excess solid in solution by centrifugation at 6240 $\times$ *g* for 30 min in a Heraeus Megafuge 1.0 centrifuge at 20 °C. The concentration of the supernatant was determined by HPLC as described above. The solid form at the end of the experiment was analyzed by DSC.

Amorphous solubility determination

Amorphous solubility of AK100 was determined with a UV–vis spectrophotometer UV-2101 PC, Shimadzu (Tokyo, Japan). AK100 solutions at different concentrations (1, 5, 10, 20 and 40 mg/mL) were prepared in DMA. Different amounts from the stock solutions, not exceeding 1 % of DMA, were added to 5 mL of water containing HPMC (76 μg/mL). Similar experiments were done in the presence of HPMC and at different concentrations of the predissolved surfactants (SDS, PS80 and TPGS). The intensity of light scattered was detected by monitoring the extinction at a non-absorbing wavelength of 540 nm as a function of the added amount of the compound. The concentration at which the scattering increased was determined as the onset of LLPS.

Preparation of amorphous solid dispersion (ASD)

Solvent evaporation was used to prepare an ASD containing AK100 and HPMC. A solution was made by dissolving a total of 500 mg of a mixture containing 80% w/w HPMC and 20% w/w AK100 in 2.3 mL of methanol, 0.3 mL DMA and 2.3 mL DCM. The solvent was removed in a rotary evaporator R-124 (BÜCHI Labortechnik AG, Switzerland) at 50 °C. The samples were then placed under vacuum for 24 h to remove any residual solvent and thereafter sealed and stored in a refrigerator. The prepared formulation was studied by DSC to confirm the amorphous nature of the material.

Dissolution of formulations

Dissolution studies were run for the prepared solid dispersion at room temperature under non-sink conditions. The powder formulation (26 mg) was added to 50 mL of water or 50 mL aqueous solution of 2 mg/mL of SDS and PS80, or 5 mg/mL TPGS. The solutions were continuously stirred at 300 rpm at room temperature using a micro magnetic stirrer bar. Three independent samples were performed at each timepoint. The amount added of the powder formulation assured that the compound was slightly above the amorphous solubility at the studied condition. Samples (200 μL) were collected at 5, 10, 15, 30, 45, 60, 90, 120, 150, and 180 min from three independent experiments. The samples were centrifuged in a Heraeus Biofuge 13 centrifuge, at 13,793 $\times$ *g* for 7 min and the concentration of the supernatant determined by HPLC.

Cell culture

Caco-2 cells obtained from American Tissue Collection, Rockville, MD were maintained in an atmosphere of 90 % air and 10 % CO_2 as described previously (Artursson, 1990). For transport experiments, 3.3×10^5 cells were seeded on polycarbonate filter inserts (12 mm diameter; pore size 0.4 μm; Costar) and allowed to grow and differentiate for 21–30 days before the cell culture monolayers were used for transport experiments.

Transport protocol

Stock solutions of AK100 at 10 mg/mL were prepared in DMA. To produce solutions above the amorphous solubility, 30 μL of stock solution was added to 3 mL (or 20 μL to 2 mL) of Hank's balanced salt solution, containing HEPES at pH 6.5 (HBSS pH 6.5). The final concentration of DMA was $\sim$1 %. The applied concentration was non-toxic to the monolayers, as assessed by integrity measurements using the paracellular marker [14C]-mannitol (57.3 mCi/mmol purchased from Perkin-Elmer Life Sciences, Boston, MA). In addition, solutions equivalent to the crystalline solubility of AK100 were generated to compare the flux at the crystalline versus amorphous solubility across Caco-2 cell monolayers.

The transport experiments ran for 60 min. They were started by the application of the drug solution to the (apical) donor side (n = 3, repeated twice except for saturated solutions which were only studied in one triplicate). The commonly used pH gradient of pH 6.5 in the apical chamber and pH 7.4 in the basolateral chamber was used to mimic absorption in the small intestine. The experiment was performed at 37 °C and the filter inserts were stirred at 500 rpm on IKA-Schüttler MTS4 to obtain data unbiased by the aqueous boundary layer. The receiver chambers were sampled continuously, with 600 μL removed for analysis at 15, 30 and 60 min. These samples were replaced with equal volumes of pre-heated receiver solution. The samples were analyzed with HPLC immediately after the experiment was terminated. As the resulting systems vary in thermodynamic activity, the only difference between them is the free drug available for membrane transport. The flux equation can be given by:

$$J = \frac{\mathrm{dM}}{\mathrm{dtA}} = \frac{\mathrm{D}\alpha}{\mathrm{h}\gamma_{\mathrm{m}}} \quad (2)$$

where J is the flux of drug molecules diffusing across the cell membrane, and (dM/dt) is the change in mass by unit time. A, D, α, γ_{m} and h are the cross-sectional area of the Caco-2 monolayer used, the diffusion coefficient of AK100, the thermodynamic activity, the activity coefficient of the drug in the membrane, and the thickness of the membrane, respectively. If A, D, α, γ_{m} and h remain constant, then

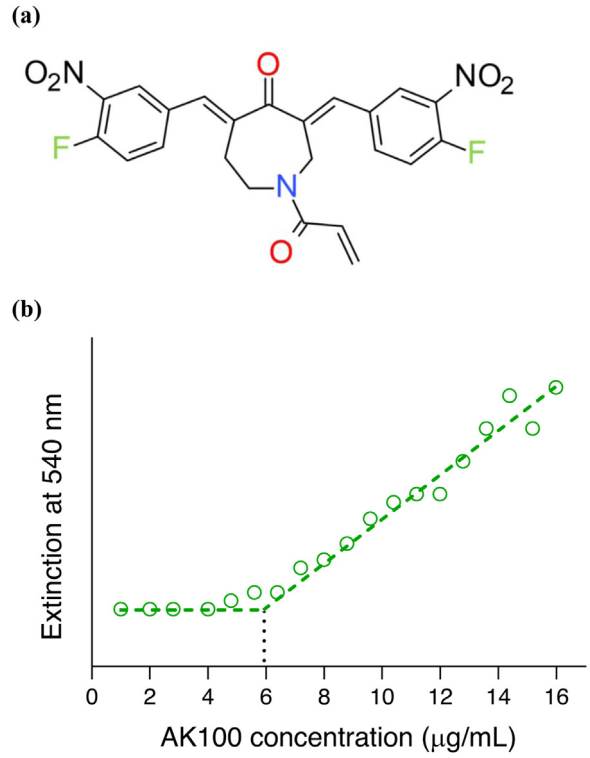

Fig. 1. a) Chemical structure of the AK100, b) Liquid–liquid phase separation (LLPS) of AK100, determined by UV extinction. Scattering increases at 540 nm when the second phase (LLPS) is generated at 6 μg/mL.

the flux is directly proportional to the thermodynamic activity (α), whereby activity is given as:

$$\alpha = \gamma C \quad (3)$$

and C is the drug concentration.

Statistical analysis

All results are expressed as mean values with the standard deviation in parentheses. Unpaired *t*-tests were used at a 95 % confidence interval to evaluate the differences between samples at 0, 2, and 5 mg/ml TPGS during the flux experiments. Values of $p < 0.05$ were considered statistically significant. The analysis was done with GraphPad Prism software (version 9.0.0).

Results

Characterization of AK100 and the ASD

Fig. 1a shows the chemical structure of AK100 and the properties of the model compound AK100 are shown in Table 1. The compound is a non-ionizable lipophilic compound with a log P of 3.3. The crystalline and amorphous solubility of AK100 in water are presented in Table 2. The AK100 maintained its stable form during the solubility studies, as confirmed by DSC analysis (Supporting Information Figure S1). Fig. 1b shows the concentration of AK100 at which the LLPS occurs, determined from the UV extinction as a function of increased concentration of the compound. The green circles represent the measured value of extinction, and the solid line indicates the onset of LLPS. The amorphous solubility of the compound was 7-fold higher than its crystalline solubility. The amorphous solubility of AK100 in aqueous solution containing 72 μg/mL HPMC was found to be 6 μg/mL. The formulation using AK100 and HPMC was confirmed to be amorphous by the disappearance of the crystalline melting peak in the DSC thermograms and the appearance of a diffuse halo in the PXRD patterns (Supporting information Figure S2).

Effect of surfactants on crystalline and amorphous solubility

The impact of solubilization by surfactants on crystalline and amorphous solubility of AK100 was investigated. The solubility of AK100 was measured in the presence of different concentrations of SDS, PS80 and TPGS. Fig. 2 shows the concentration of AK100 in crystalline and amorphous forms as a function of increased concentrations of surfactants. The amorphous solubility was higher than the crystalline solubility at all measured ranges and in the three different surfactants. The efficiency of solubilization by the surfactants varied; the crystalline solubility of AK100 was 49 μg/mL, 13 μg/mL, and 54 μg/mL in 6 mg/mL pre-dissolved SDS, PS80 and TPGS, respectively. These amounts corresponded to 21, 5 and 14 mM of SDS, PS80 and TPGS, respectively.

Dissolution of the amorphous solid dispersion

Dissolution studies of the prepared ASD were performed to determine the maximum achievable concentration and solution behavior of AK100 in different surfactants. As seen in Fig. 3a, the maximum concentration of AK100 achievable in water was comparable with the amorphous solubility determined using UV–vis spectroscopy (6 μg/mL). The dispersion formed turbid solutions within a few minutes of addition to water and maintained supersaturation for the duration of the experiment (180 min). Dissolution profiles of the ASD in presence of SDS, PS80 and TPGS are presented in Fig. 3. The concentration of AK100 was not stable in presence of SDS and PS80, while it maintained its concentration (80 μg/mL) for 180 min in TPGS.

Membrane transport

The cell-based study was conducted to explore the impact of surfactant concentration and solubilization on membrane transport of AK100 through a biologically relevant membrane. Fig. 4 shows the flux for the AK100 from its crystalline and amorphous solutions in water and predissolved TPGS. The flux of amorphous material was higher than that observed from the crystalline form in all studied conditions. Indeed, it was not possible to detect any flux generated by the crystalline form in water. On the other hand, the flux of amorphous AK100 was determined to be 0.004 mg/min/cm^2 and 0.0016 mg/min/cm^2 in 2 mg/mL and 5 mg/mL of TPGS, respectively. The flux of the AK100 in amorphous form (2 mg/mL in TPGS) was about 1.6 times higher than that of its crystalline form (5 mg/mL TPGS).

Table 1
Physicochemical properties of the drug AK100.

Drug	Ionization	pK_a	MW (g.mol^{-1})	log P	ΔH_f (KJ.mol^{-1})	T_m (K)	T_g (K)
AK100	neutral	–	469.39	3.3	48.8	393	301

pK_a: acid dissociation constant, MW: molecular weight, log P: log partition coefficient between octanol and water, ΔH_f: of heat of fusion, T_m: onset of melting and T_g: glass transition temperature at inflection.

Table 2
Crystalline and amorphous solubility of AK100 in water; the standard deviation based on six replicates is shown in parentheses.

Drug	Crystalline solubility (μg/mL)	Amorphous solubility (μg/mL)	Amorphous advantage S_A/S_C[a]
AK100	0.86 (0.1)	6	7.5

[a] S_A/S_C: ratio of amorphous to crystalline solubility.

Discussion

ASD is a strategy to increase the bioavailability of poorly soluble compounds. The amorphous material has higher solubility and activity than the crystalline counterpart and thereby improves the solubility and flux of the compounds.[31] The major challenge in amorphous formulation development is that the material is thermodynamically unstable and tends to crystallize.[32,33] To prevent this, polymers are used to stabilize the drugs in solution and solid states. Other excipients might be added to the formulation to improve solubility, such as surfactants above their critical micelle concentration.

It is well-known that crystal packing and hydrophobicity of the compound are major barriers for drug solubility in crystalline form. The free energy of solution can be described as follows in relation of crystal and solvation contributions[34]

$$\Delta G_{solution} = \Delta G_{fusion} + \Delta G_{solvation} \quad (4)$$

Therefore, the addition of a solubilizing agent impacts only the solvation contribution (γ) which can be evaluated from the following equation:

$$\log X = \log X_{ideal} - \log\gamma \quad (5)$$

where X is the measured aqueous solubility under nonionizing conditions, X_{ideal} is the calculated ideal solubility, and γ is the activity coefficient of the solute in water.

X_{ideal} can be approximated from the following equation:

$$X_{ideal} = \frac{-\Delta H_m}{R}\left(\frac{T_m - T}{T_m T}\right) \quad (6)$$

where ΔH_m, T_m, R, and T are the melt enthalpy, the melt temperature, the ideal gas constant, and the experimental temperature (310 K), respectively. Eq. (6) assumes that the heat capacity change upon melting is zero and that the enthalpy of the solution is equal to the ΔH_m. Fig. 5 summarizes the contribution of the crystal packing and the activity coefficient as barriers to the solubility of AK100. The bars in the negative side of the x-axis are split into two portions—black and grey—corresponding to the crystal packing and the solvation contribution, respectively. Upon adding surfactants, the solubility of the drug increases by micellar solubilization which depends on the drug and the surfactant properties as well as the concentration of the surfactant in solution. The solubility enhancement achieved by the addition of the surfactant in Fig. 5 causes a decrease in the activity coefficient (grey portion of the bar) which is reduced as a function of increased concentration of the surfactant.

Effect of surfactant on crystalline and amorphous solubility

The partitioning of the drug between the micellar phase and the aqueous free drug phase can be defined by the micellar partition coefficient (K_m) at crystalline and amorphous solubility. This coefficient is defined as the ratio of the surfactant-associated drug concentration to that of the free drug in the aqueous phas:e[6,22,23,35]

$$K_m = \frac{C_m}{S_0} \quad (7)$$

where C_m is the difference of the drug solubility in the presence and absence of the surfactant and S_0 is drug solubility in absence of surfactant, assuming that the surfactant does not mix with the solid phases and the free drug concentration is the same in the complex media as it is without excipients. Plotting the K_m of the surfactants as a function of the surfactant concentration gives the solubilisation capacity of each surfactant at crystalline and amorphous solubility for AK100 (Fig. 6).

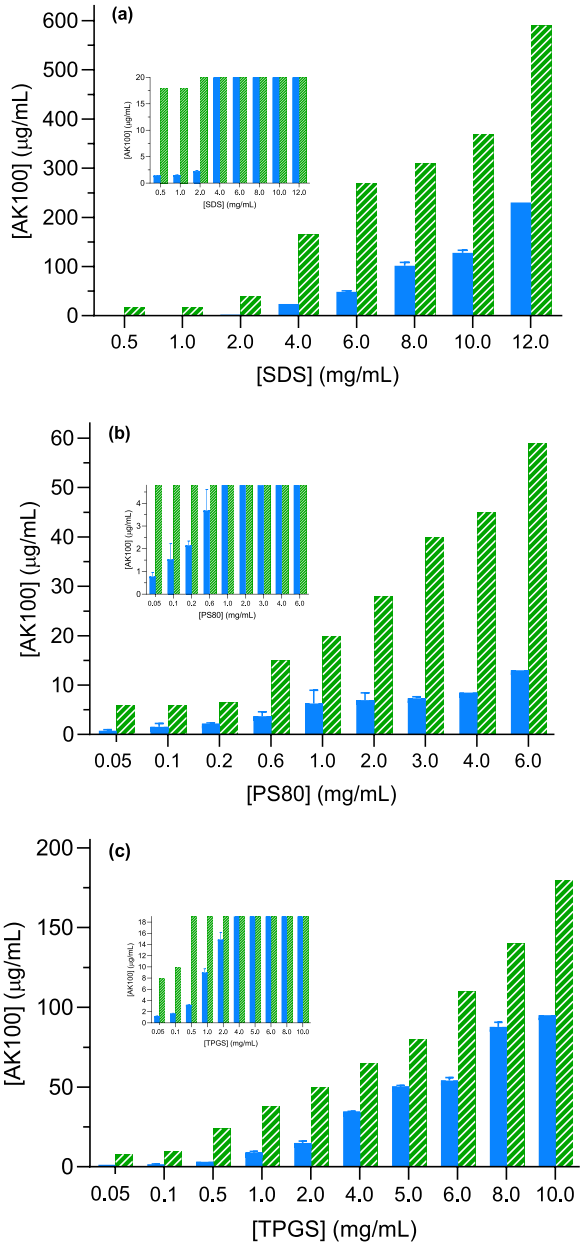

Fig. 2. Crystalline (solid, blue) and amorphous (striped, green) solubilities of AK100 in the presence of different concentrations of: (a) SDS, (b) PS80 and (c) TPGS. Error bars represent crystalline solubility measurements of three replicates.(For interpretation of the references to color in this figure legend, the reader is referred to the web version of this article.)

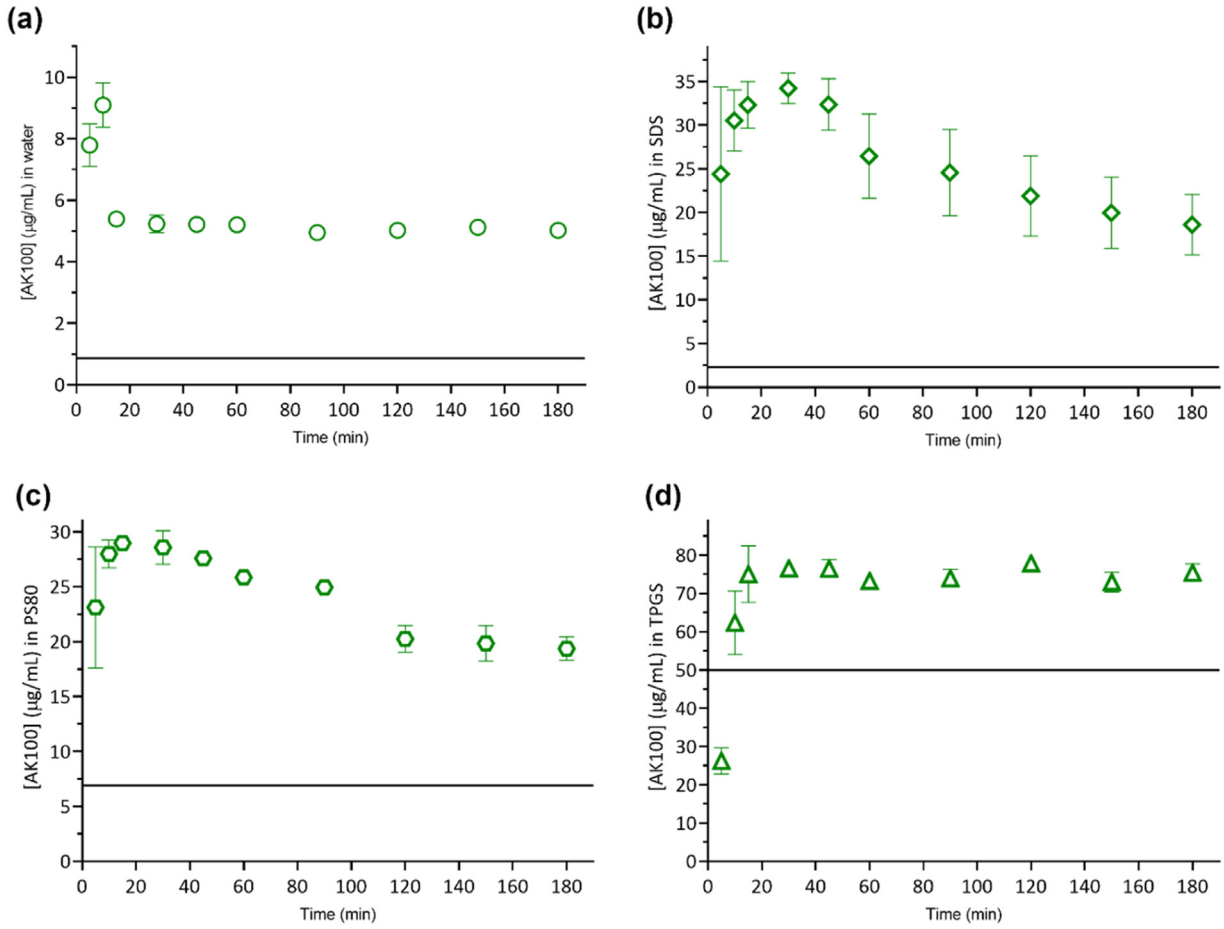

Fig. 3. Powder dissolution profiles of formulations containing 80 % HPMC and 20 % AK100 dissolved in: (a) water, (b) 2 mg/ml SDS, (c) 2 mg/ml PS80 and (d) 5 mg/ml TPGS. Solid line represents solubility of crystalline form in the presence of surfactant. Error bars (three replicates) indicate the standard deviation.

The K_m was different for the three surfactants studied. The K_m value at crystalline solubility was higher than that of the amorphous solubility when the concentration of the surfactant exceeded 8 mg/mL (SDS) and 1 mg/mL (TPGS). In contrast, the K_m of PS80 was lower at the amorphous solubility than at the crystalline solubility at all studied concentrations. In a recent study, the K_m of different physiological fluids (micellar solubilization) was lower at amorphous solubility than at crystalline solubility of two structurally diverse compounds, atazanavir and posaconazole.[22] These results agree with ours when the concentration of the surfactants exceeded certain limits. The higher K_m at amorphous solubility of AK100 at low surfactant concentration can be explained by the dilution of the system.

The increase of the solubility of the crystalline and amorphous material was considered linear as a function of increased surfactant concentration (Fig. 7). Thus, the solubility of a solute at a certain surfactant concentration (S_{total}) can be simply predicted using the following equation[36]

$$S_{total} = S_0\ (1 + K_s[M]) \quad (8)$$

where S_0 is the drug solubility in the aqueous phase, K_S is the micellar solubilization constant which should be independent of the solute and surfactant concentration, and [M] is the surfactant micellar concentration. The K_s value of the surfactant is an indication of the solubilization capacity of the surfactant. K_s can be evaluated from the slope of the solubilization curve and expressed as:

$$K_S = \frac{C_m}{S_0[M]} \quad (9)$$

where, C_m is the drug solubility at any surfactant micellar concentration.

The slope of the relation between the solubility of drug and the concentration of surfactant was evaluated for each surfactant at crystalline and amorphous solubility (Table 3). The relation was linear and the linearity at amorphous solubility had a higher coefficient of determination (R^2) value than that at crystalline solubility. This was as expected because the solubility of crystalline material is an interplay between crystallinity and hydrophobicity of the molecules, which impacts the linear fitting. The K_S values at crystalline solubility were always higher than those at amorphous solubility for the three surfactants. K_S was found to vary between crystalline and amorphous material. This was also observed for cocrystals of other drugs in previous studies, where the K_S was reported to vary between different cocrystal forms of a drug.[37,38] However, a cocrystal is a multicomponent system and its response to surfactants is not linearly dependent on the micellar concentration of the surfactant.

Amorphous solubility increased linearly with increased surfactant concentration. This indicates that the amount of surfactant in solution did not negatively affect the solubility of the drug as do some polymers. For example, at high concentrations in solution, HPMC based polymers may decrease the amorphous solubility by partitioning into the drug-rich phase.[14,39–41] This was not the case for the surfactants studied here at the ranges of concentration used.

Dissolution and membrane transport

Maintaining supersaturation during the course of absorption is essential for achieving the solubility advantages offered by the

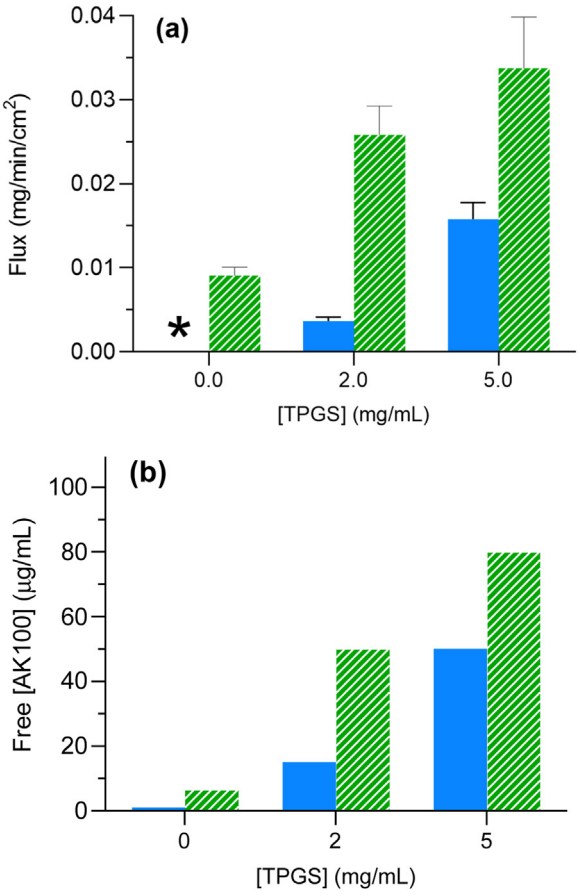

Fig. 4. Flux measurements of the crystalline (solid, blue) and amorphous (striped, green) forms of AK100 at different concentrations of TPGS. Error bars represent crystalline solubility measurements of three replicates.

* value below the LCMS limit of detection. (b) concentration of free AK100 in the (apical) donor side of the setup.(For interpretation of the references to color in this figure legend, the reader is referred to the web version of this article.)

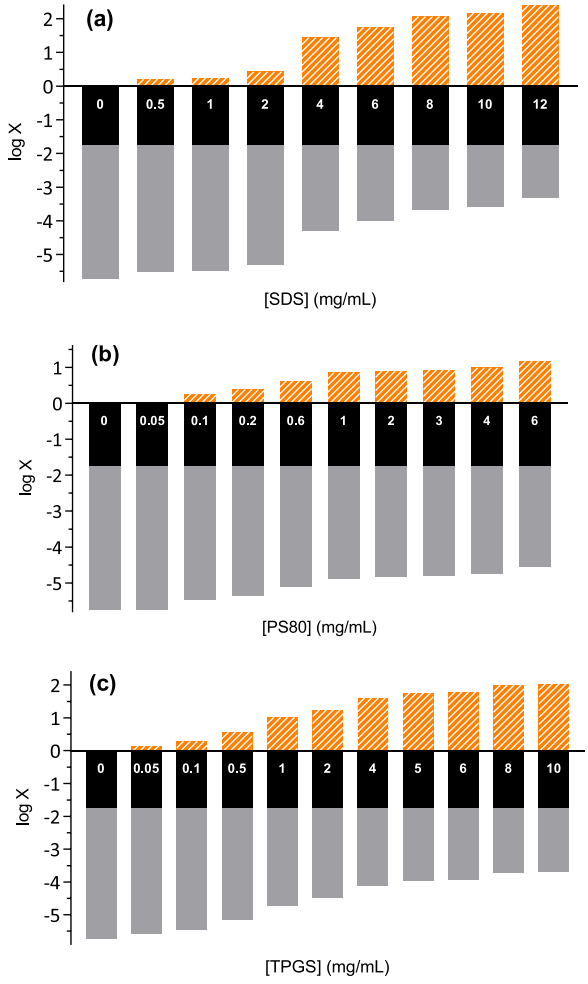

Fig. 5. Solubility enhancement with different concentrations of (a) SDS, (b) PS80 and (c) TPGS. The striped, orange portion of the bars represents the solubility enhancement achieved by the addition of the surfactants. Also shown are the two factors, independent of each other, that determine solubility: the ideal solubility (black) and the activity coefficient (grey).(For interpretation of the references to color in this figure legend, the reader is referred to the web version of this article.)

amorphous formulation.[42] The supersaturation of AK100 (without surfactants) was maintained for 180 min. In presence of SDS and PS80, supersaturation decreased after 60 min, which may have been because the surfactants triggered nucleation and crystallization of the drug (Figs. 4 and 5). On the other hand, TPGS did not lower the supersaturation of AK100. Similar to our observations, a previous study of an ASD of celecoxib reports that SDS and PS80 enhanced the crystallization of the drug. The authors attribute this to the unbranched structures of SDS and PS80 since surfactants with branched chemical structures did not trigger crystallization.[21] In our study the TPGS was shown in this study to not impact the supersaturation for the entire period of the dissolution study. It is important to note that the AK100 was supersaturated for up to 180 min in the absence of any surfactant. This emphasizes the importance of selecting appropriate excipients during formulation development especially for surfactants which are a widely used excipient in pharmaceutical formulations. Since the dissolution profile of the ASD in the presence of TPGS showed maintained drug supersaturation and TPGS did not negatively impact the time course of supersaturation, TPGS was further selected for a flux study. The study was performed using Caco-2 cell monolayer for saturated and supersaturated solutions of AK100 in absence and presence of 2 mg/mL and 5 mg/mL TPGS. It was clear that supersaturated solutions had higher flux compared to the saturated ones, which is driven by the higher thermodynamic activity of the amorphous form of the drug compared to the crystalline counterpart. The flux of AK100 here was driven by the activity of the solid phase rather than the amount dissolved in the solution. It should be noted that the amorphous solubility of AK100 at 2 mg/mL of TPGS was similar to that of crystalline solubility at 5 mg/mL TPGS. However, the flux for the amorphous form was higher than that for the crystalline form. This shows the benefit of using the amorphous form rather than the crystalline one in toxicity studies where the amount of excipients in the formulation can affect toxicity of the total formulation.

The supersaturation of the solute can be determined from the maximum supersaturation ratio (SR_{conc}) by using concentration measurements of a supersaturated and a saturated solution as demonstrated in the following equation[22,23,43]

$$SR_{conc} = \frac{S_{amorph}}{S_{cryst}} \tag{10}$$

where S_{amorph} is the drug amorphous solubility in the same media used to measure S_{cryst}, the drug crystalline solubility. SR can also be determined based on the activity, that is the ratio of the diffusive flux of the solute at the amorphous solubility, J_{amorph}, to the diffusive flux at the crystalline solubility, J_{cryst}, as shown in the equation:

$$SR_{activity} = \frac{J_{amorph}}{J_{cryst}} \tag{11}$$

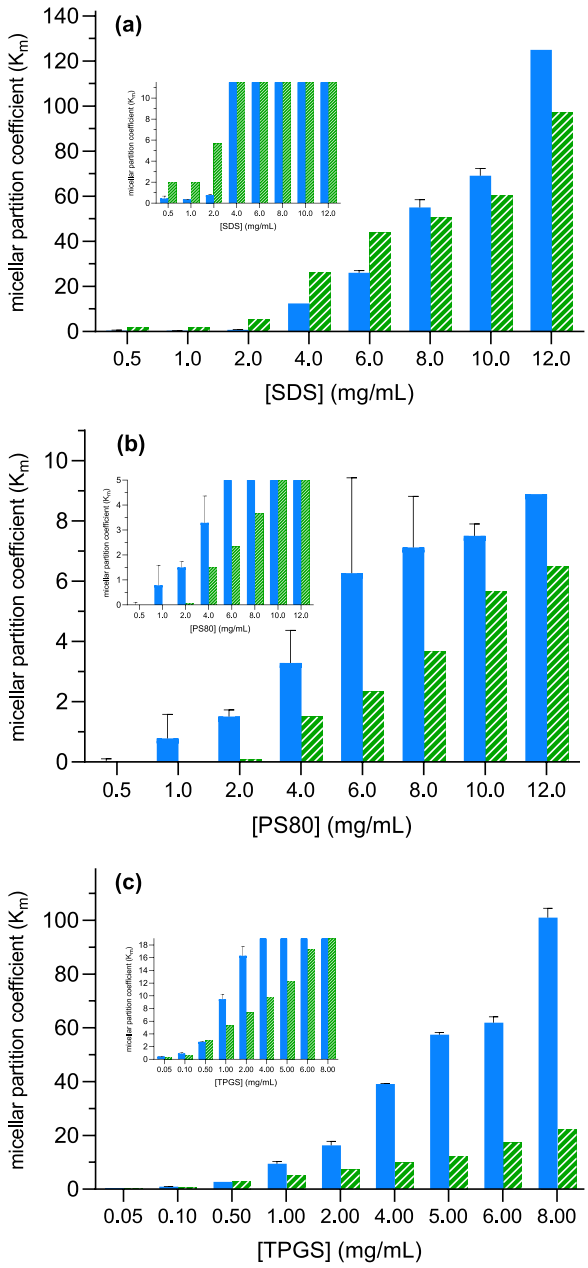

Fig. 6. Micellar partition coefficient (K_m) values at crystalline (solid, blue) and amorphous (striped, green) solubility of AK100 at different concentrations of (a) SDS, (b) PS80 and (c) TPGS. Error bars represent crystalline solubility measurements of three replicates.(For interpretation of the references to color in this figure legend, the reader is referred to the web version of this article.)

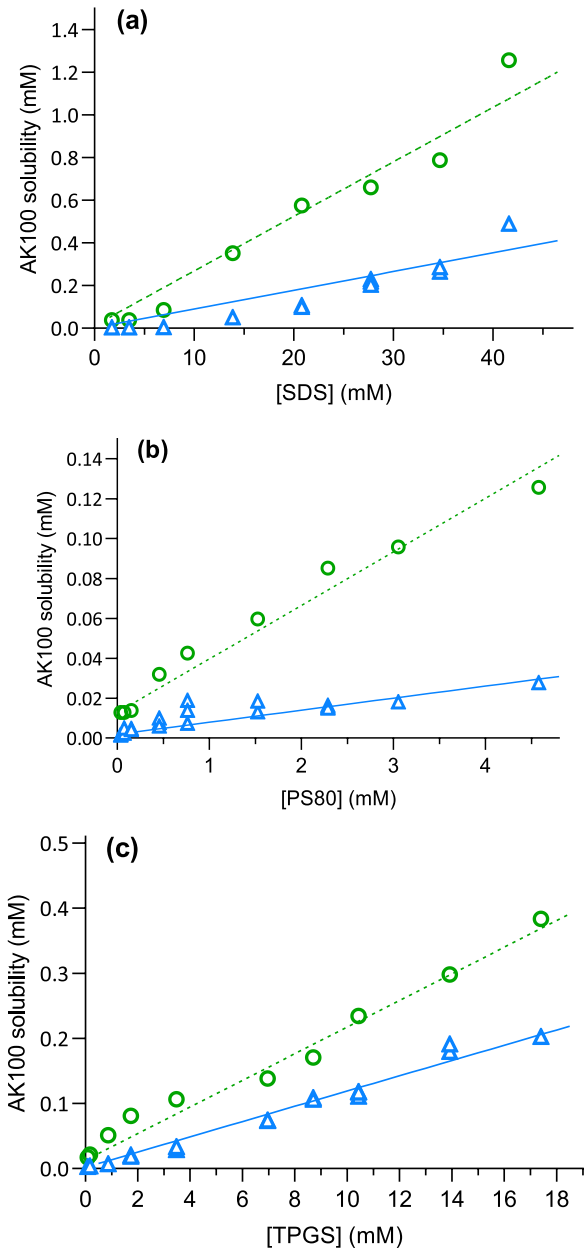

Fig. 7. Experimental and predicted solubilities of AK100 at different concentrations of (a) SDS, (b) PS80 and (c) TPGS. Measured crystalline (blue triangle) and amorphous (green circle) solubilities. Predicted crystalline (solid blue line) and amorphous solubilities (dashed green line), calculated according to Eq. (8) with Ks values from Table 3. (For interpretation of the references to color in this figure legend, the reader is referred to the web version of this article.)

Fig. 8 shows the supersaturation ratio for AK100 in presence of TPGS obtained by using either the activity-based ratio or the concentration-based one. The activity-based ratio was higher than that concentration-based one at all concentrations of TPGS. The thermodynamic activity of a drug is usually higher in concentrated solutions (amorphous form, supersaturated solution) than in diluted ones (crystalline form, saturated solution) ones. This is due to the increased complexity and non-ideality of the supersaturated solutions. On the other hand, the TPGS solubilizes the drug through micellar solubilization, which can lead to an increase in the total drug concentration and to a decrease in the thermodynamic activity of the free drug. These findings are also reported by other researchers who have found that concentration-based calculations are often misleading and underpredict the

Table 3
K_s values for AK100 at the crystalline and amorphous solubilities in the presence of three surfactants.

Surfactant	Ks_{CS} (mM^{-1})	R^2	Ks_{AS} (mM^{-1})	R^2
SDS	4.8	0.90	2.0	0.96
PS80	3.3	0.86	2.1	0.97
TPGS	6.4	0.99	1.6	0.98

K_S: micellar solubilization constant, Ks_{CS}: Ks at crystalline solubility, Ks_{AS}: Ks at amorphous solubility, R^2: coefficient of determination SDS: sodium dodecyl sulphate PS80: polysorbate 80 and TPGS: D-α-tocopherol polyethylene glycol succinate.

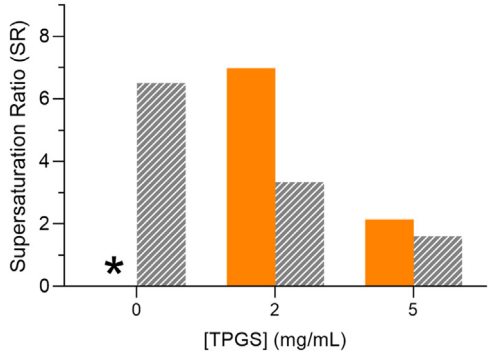

Fig. 8. Maximum supersaturation ratio (SR) for AK100 in different concentrations of TPGS, obtained using the activity-based ratio calculation (orange bars) versus the concentration-based ratio calculation (striped, grey bars). * value below the LCMS limit of detection.(For interpretation of the references to color in this figure legend, the reader is referred to the web version of this article.)

fundamental supersaturation.[23] In two different studies, the $SR_{activity}$ for atazanavir is constant as a function of surfactant concentration and in different simulated physiological fluids.[22,23] In contrast, posaconazole shows statistically significant differences among the $SR_{activity}$ values in some of the studied simulated physiological fluids.[22] Similar to these published studies, the $SR_{activity}$ of AK100 was higher than the SR_{conc} at the studied conditions. The AK100 had a similar performance as posaconazole in that $SR_{activity}$ was not constant—it varied depending on the TPGS concentration. Notably, unlike atazanavir, AK100 and posaconazole were affected by the surfactant concentration. Increased concentration of TPGS results in improved bioavailability, which is due to particle size reduction.[24] It may also be due to the ability of the surfactant to act as a permeability enhancer for the drug.[25,26]

It is also known that different excipients participate differently in the drug-rich phase, which in turn influences the supersaturation and the *SR*. In a recent study by Ueda et al., HPMC was found to be an efficient inhibitor of the coarsening of drug-rich phase particles. Indeed, mixing of the polymer and surfactants with the drug-rich phase reduces the thermodynamic activity of ketoprofen.[44] Surfactants are widely used in pharmaceutical products and physiological fluids use common micellar solubilization mechanisms, thereby complicating the process of predicting ASD performance. Thus, it is essential to better control and understand ASD behavior during drug development for ensuring efficacy and avoiding toxicity of amorphous-based formulation.

Conclusion

Excipients may alter solubility, stability, and membrane transport and thus bioavailability of amorphous formulation of drugs. This study investigates how various surfactants included in the formulation of a poorly water-soluble drug, AK100, could affect its dissolution, supersaturation, and membrane transport. The surfactants increased the solubility for crystalline and amorphous forms linearly; however, the amorphous solubility was always higher than that of the crystalline counterpart. The solubilization capacity of the surfactants varied and the capacity was higher for the crystalline form than the amorphous one. These differences were possible to predict with a mathematical model. All three surfactants PS80, SDS and TPGS improved the supersaturation but only the most branched of them, TPGS, could maintain it for 180 min. The flux determined with the Caco-2 cell model was always higher for amorphous than crystalline material and increased with increased concentration of surfactant. Finally, the relative supersaturation from the activity-based calculation was always higher than that of the concentration-based one. These results clearly demonstrate the importance of properly selecting excipients for amorphous formulations to ensure successful delivery of drugs.

Associated content

Supporting Information includes characterization of the crystalline form of AK100 and the formulation containing 80 % HPMC and 20 % AK100 by PXRD; DSC thermogram showing the melting point of AK100 before and after crystalline solubility determination; and DSC thermogram of the amorphous solid dispersion containing 80 % HPMC and 20 % AK100.

Declaration of competing interest

The authors declare that they have no known competing financial interests or personal relationships that could have appeared to influence the work reported in this paper.

Acknowledgments

The authors acknowledge Uppsala University and Recipharm OT Chemistry who jointly participated in the study design and review of this publication. The authors also acknowledge the Swedish Foundation for Strategic Research for providing financial support for the PhD project of M.E.S.; Grant no. 17-0100.

Supplementary materials

Supplementary material associated with this article can be found in the online version at doi:10.1016/j.xphs.2024.10.023.

References

1. Shah SM, Jain AS, Kaushik R, Nagarsenker MS, Nerurkar MJ. Preclinical formulations : insight, strategies, and practical considerations. *AAPS PharmSciTech*. 2014;15(5). https://doi.org/10.1208/s12249-014-0156-1.
2. Psimadas D, Georgoulias P, Valotassiou V, Loudos G. Materials science tetrahedron—a useful tool for pharmaceutical research and development. *J Pharm Sci*. 2012;101(7):2271–2280. https://doi.org/10.1002/jps.
3. Neervannan S. Preclinical formulations for discovery and toxicology: physicochemical challenges. *Expert Opin Drug Metab Toxicol*. 2006;2(5):715–731. https://doi.org/10.1517/17425255.2.5.715.
4. Alskär LC, Keemink J, Johannesson J, Porter CJH, Bergström CAS. Impact of drug physicochemical properties on lipolysis-triggered drug supersaturation and precipitation from lipid-based formulations. *Mol Pharm*. 2018;15(10):4733–4744. https://doi.org/10.1021/acs.molpharmaceut.8b00699.
5. Kawakami K, Oda N, Miyoshi K, Funaki T, Ida Y. Solubilization behavior of a poorly soluble drug under combined use of surfactants and cosolvents. *Eur J Pharm Sci*. 2006;28(1–2):7–14. https://doi.org/10.1016/j.ejps.2005.11.012.
6. Li P, Tabibi SE, Yalkowsky SH. Solubilization of ionized and un-ionized flavopiridol by ethanol and polysorbate 20. *J Pharm Sci*. 1999;88(5):507–509. https://doi.org/10.1021/js980433. o.
7. Taylor LS, Zhang GGZ. Physical chemistry of supersaturated solutions and implications for oral absorption. *Adv Drug Deliv Rev*. 2016;101:122–142.
8. Newman A.W., Childs S.L., Cowans B.A. Salt and cocrystal form selection. *Preclinical Development Handbook: ADME and Biopharmaceutical Properties*. Published online 2008:455–481. doi:10.1002/9780470249031.ch14.
9. Good DJ, Rodríguez-Hornedo N. Solubility advantage of pharmaceutical cocrystals. *Cryst Growth Des*. 2009;9(5):2252–2264.
10. Alhalaweh A, Ali HRH, Velaga SP. Effects of polymer and surfactant on the dissolution and transformation profiles of cocrystals in aqueous media. *Cryst Growth Des*. 2014;14(2):643–648. https://doi.org/10.1021/cg4015256.
11. Pandi P, Bulusu R, Kommineni N, Khan W, Singh M. Amorphous solid dispersions: an update for preparation, characterization, mechanism on bioavailability, stability, regulatory considerations and marketed products. *Int J Pharm*. 2020;586(May):119560. https://doi.org/10.1016/j.ijpharm.2020.119560.
12. Hancock BC, Shamblin SL, Zografi G. Molecular mobility of amorphous pharmaceutical solids below their glass transition temperatures. *Pharm Res Off J Am Assoc Pharm Sci*. 1995;12(6):799–806. https://doi.org/10.1023/A:1016292416526.
13. Edueng K, Mahlin D, Larsson P, Bergström CAS. Mechanism-based selection of stabilization strategy for amorphous formulations : insights into crystallization pathways. *J Control Rel*. 2017;256:193–202.

14. El Sayed M, Alhalaweh A, Bergström CA. Insights into dissolution and solution chemistry of multidrug formulations of antihypertensive drugs. *Mol Pharm*. 2020;17(10):4018–4028. https://doi.org/10.1021/acs.molpharmaceut.0c00835.
15. El Sayed M, Alhalaweh A, Bergström CAS. Impact of simulated intestinal fluids on dissolution, solution chemistry, and membrane transport of amorphous multidrug formulations. *Mol Pharm*. 2021;18(11):4079–4089. https://doi.org/10.1021/acs.molpharmaceut.1c00480.
16. Ilevbare GA, Taylor LS. Liquid-liquid phase separation in highly supersaturated aqueous solutions of poorly water-soluble drugs: implications for solubility enhancing formulations. *Cryst Growth Des*. 2013;13(4):1497–1509. https://doi.org/10.1021/cg301679h.
17. Mosquera-Giraldo LI, Taylor LS. Glass-liquid phase separation in highly supersaturated aqueous solutions of telaprevir. *Mol Pharm*. 2015;12(2):496–503. https://doi.org/10.1021/mp500573z.
18. Almeida L, Reutzel-edens SM, Stephenson GA, Taylor LS. Assessment of the amorphous " solubility " of a group of diverse drugs using new experimental and theoretical approaches. *Mol Pharm*. 2015;12:484–495. https://doi.org/10.1021/mp500571m.
19. Indulkar AS, Mo H, Gao Y, Raina SA, Zhang GGZ, Taylor LS. Impact of micellar surfactant on supersaturation and insight into solubilization mechanisms in supersaturated solutions of Atazanavir. *Pharm Res*. 2017;34(6):1276–1295. https://doi.org/10.1007/s11095-017-2144-0.
20. Ilevbare GA, Taylor LS. Liquid-liquid phase separation in highly supersaturated aqueous solutions of poorly water-soluble drugs: implications for solubility enhancing formulations. *Cryst Growth Des*. 2013;13(4):1497–1509. https://doi.org/10.1021/cg301679h.
21. Chen J, Ormes JD, Higgins JD, Taylor LS. Impact of surfactants on the crystallization of aqueous suspensions of celecoxib amorphous solid dispersion spray dried particles. *Mol Pharm*. 2015;12(2):533–541. https://doi.org/10.1021/mp5006245.
22. Elkhabaz A, Moseson DE, Brouwers J, Augustijns P, Taylor LS. Interplay of supersaturation and solubilization: lack of correlation between concentration-based supersaturation measurements and membrane transport rates in simulated and aspirated human fluids. *Mol Pharm*. 2019(1). https://doi.org/10.1021/acs.molpharmaceut.9b00956.
23. Indulkar AS, Mo H, Gao Y, Raina SA, Zhang GGZ, Taylor LS. Impact of micellar surfactant on supersaturation and insight into solubilization mechanisms in supersaturated solutions of Atazanavir. *Pharm Res*. 2017;34(6):1276–1295. https://doi.org/10.1007/s11095-017-2144-0.
24. Kesisoglou F, Wang M, Galipeau K, Harmon P, Okoh G, Xu W. Effect of amorphous nanoparticle size on bioavailability of anacetrapib in dogs. *J Pharm Sci*. 2019;108(9):2917–2925. https://doi.org/10.1016/j.xphs.2019.04.006.
25. Xia W, Hayat Onyuksel H. Mechanistic studies on surfactant-induced membrane permeability enhancement. *Pharm Res*. 2000;17:612–618.
26. Swenson ES, Milisen W, Curatolo W. Intestinal permeability enhancement: efficacy, acute local toxicity, and reversibility. *Pharm Res*. 1994;11:1132–1142.
27. Hubatsch I, Ragnarsson EGE, Artursson P. Determination of drug permeability and prediction of drug absorption in Caco-2 monolayers. *Nat Protoc*. 2007;2(9):2111–2119. https://doi.org/10.1038/nprot.2007.303.
28. Behrens I, Stenberg P, Artursson P, Kissel T. Transport of lipophilic drug molecules in a new mucus-secreting cell culture model based on HT29-MTX cells. *Pharm Res*. 2001;18(8):1138–1145. https://doi.org/10.1023/A:1010974909998.
29. Artursson P, Palm K, Luthman K. Caco-2 monolayers in experimental and theoretical predictions of drug transport. *Adv Drug Deliv Rev*. 2012;64:280–289. https://doi.org/10.1016/j.addr.2012.09.005.
30. A.G. Huesgen. *Agilent Application Note: determination of Log P for Compounds of Different Polarity the Agilent 1200 Infinity Series Impurity Analyzer System*.; 2019.
31. Schittny A, Huwyler J, Puchkov M. Mechanisms of increased bioavailability through amorphous solid dispersions: a review. *Drug Deliv*. 2020;27(1):110–127. https://doi.org/10.1080/10717544.2019.1704940.
32. Alonzo DE, Zhang GGZ, Zhou D, Gao Y, Taylor LS. Understanding the behavior of amorphous pharmaceutical systems during dissolution. *Pharm Res*. 2010;27(4):608–618.
33. Gupta P, Thilagavathi R, Chakraborti AK, Bansal AK. Role of molecular interaction in stability of celecoxib-PVP amorphous systems. *Mol Pharm*. 2005;2(5):384–391. https://doi.org/10.1021/mp050004g.
34. Miyako Y, Tai H, Ikeda K, Kume R, Pinal R. Solubility screening on a series of structurally related compounds : cosolvent-induced changes on the activity coefficient of hydrophobic solutes solubility screening on a series of structurally related compounds : cosolvent-induced changes on the activity coefficient of hydrophobic solutes. *Drug Dev Ind Pharm*. 2008;34:499–505. https://doi.org/10.1080/03639040701744020.
35. He Y, Tabibi SE, Yalkowsky SH. Solubilization of two structurally related anticancer drugs: XK-469 and PPA. *J Pharm Sci*. 2006;95(1):97–107. https://doi.org/10.1002/jps.20500.
36. Huang Y, Dai WG. Fundamental aspects of solid dispersion technology for poorly soluble drugs. *Acta Pharm Sin B*. 2014;4(1):18–25.
37. Alhalaweh A, Ali HRH, Velaga SP. Effects of polymer and surfactant on the dissolution and transformation profiles of cocrystals in aqueous media. *Cryst Growth Des*. 2014;14(2):643–648. https://doi.org/10.1021/cg4015256.
38. Good DJ, Rodríguez-Hornedo N. Solubility advantage of pharmaceutical cocrystals. *Cryst Growth Des*. 2009;9(5):2252–2264.
39. Ueda K, Taylor LS. Polymer type impacts amorphous solubility and drug-rich phase colloidal stability: a mechanistic study using nuclear magnetic resonance spectroscopy. *Mol Pharm*. 2024. Published online 2020.
40. Ueda K, Hate SS, Taylor LS. Impact of hypromellose acetate succinate grade on drug amorphous solubility and in vitro membrane transport. *J Pharm Sci*. 2020:1–10. Published online.
41. Li N, Taylor LS. Tailoring supersaturation from amorphous solid dispersions. *J Control Rel*. 2018;279:114–125.
42. Newman A, Reutzel-Edens SM, Zografi G. Coamorphous active pharmaceutical ingredient–small molecule mixtures: considerations in the choice of coformers for enhancing dissolution and oral bioavailability. *J Pharm Sci*. 2018;107(1):5–17. https://doi.org/10.1016/j.xphs.2017.09.024.
43. Mullin J.W. Solutions and solubility. *Crystallization*. 2001;(2001):86–134. doi:10.1016/b978-075064833-2/50005-x.
44. Ueda K, Taylor LS. Partitioning of surfactant into drug-rich nanodroplets and its impact on drug thermodynamic activity and droplet size. *J Control Rel*. 2021;330:229–243. https://doi.org/10.1016/j.jconrel.2020.12.018.